Available online at www.sciencedirect.com
ScienceDirect
Polymer 48 (2007) 5702–5712
polymer
www.elsevier.com/locate/polymer

Mechanical properties, morphology and molecular characteristics of poly(ethylene terephthalate) toughened by natural rubber

P. Phinyocheep [a,b,*], J. Saelao [a], J.Y. Buzaré [c,d]

[a] Department of Chemistry, Faculty of Science, Mahidol University, Rama VI Road, Phayathai, Bangkok 10400, Thailand
[b] Institute of Science and Technology for Research and Development, Salaya Campus, Mahidol University, Nakornpathom 73170, Thailand
[c] Laboratoire de Physique de l'Etat Condensé (UMR CNRS 6087), Faculté des Sciences, Université du Maine, Le Mans, France
[d] Institut de Recherche en Ingénierie Moléculaire et Matériaux Fonctionnels (FR CNRS2575), Université du Maine, Le Mans, France

Received 5 February 2007; received in revised form 25 June 2007; accepted 4 July 2007
Available online 15 July 2007

Abstract

The melt blending of poly(ethylene terephthalate) (PET) and natural rubber (NR) in a twin-screw extruder is studied. Parameters affecting the blend properties such as the amounts of the NR in the blends and screw speeds are investigated. Increased toughness of the PET/NR blend was found as the amount of NR was increased. The impact strength of the PET/NR (80/20 wt%) blend using a screw speed of 100 rpm, increased up to seven-fold when compared to that of pure PET. The morphology of the blend was investigated by SEM. The molecular characteristic was evaluated by spectroscopic technique. The toughening effect of NR on the PET might come from the possible interaction between the two phases, which was clearly evidenced by solid-state CP/MAS ^{13}C NMR data. The data revealed an increase in the cross polarization time (T_D) of the carbonyl carbon and a decrease of the $T_{1\rho}^{H}$ relaxation of the carbonyl groups in the PET/NR blend. This should come from the interaction between the carbonyl group of PET with some abnormal groups such as hydroxyl function in the NR, resulting in an improvement of the compatibility of the studied blends.

Keywords: PET/NR blend; Solid-state CP/MAS ^{13}C NMR; Molecular characteristic

1. Introduction

Poly(ethylene terephthalate) (PET) is an important engineering thermoplastic polyester because of its good combination of properties, such as having good thermal and mechanical properties as well as having excellent chemical resistance, good optical and barrier properties. However, the notched impact strength of PET is very low, a property not desired in engineering thermoplastics, e.g., polyamides. The improvement of the notched impact behavior can be done by incorporating an elastomeric material in it. The basis of the improvement is the better dispersion of small rubber particles in the polymer matrix. Based on theories on rubber toughening [1], the blend morphologies and characteristics such as the average rubber particle size and the concentration of the dispersed phase, will have distinct influences on the final mechanical behaviors. Parameters influencing the phase morphology development and the impact response of rubber toughened polymers are the type and content of the rubber, the type and content of the reactive compatibilizer, the viscosity ratio and the mixing conditions [2,3]. A finely dispersed rubber phase, at the submicron level, is often a prerequisite for obtaining the desired notched impact response.

PET has been blended with various elastomers such as EPR, EPDM, NBR and SBR. Due to the difference in their polarity, they are often immiscible. This results in unfavorable mechanical properties [4–10]. Functionalization of elastomers such as ABS [11], EPR [4–7], EPDM [5], NBR [5], SBR [8] and SEBS [10,12] with reactive functionalities, i.e., maleic

* Corresponding author. Department of Chemistry, Faculty of Science, Mahidol University, Rama VI Road, Phayathai, Bangkok 10400, Thailand. Tel.: +66 02 201 5167; fax: +66 02 354 7151.
E-mail address: scppo@mahidol.ac.th (P. Phinyocheep).

0032-3861/$ - see front matter © 2007 Elsevier Ltd. All rights reserved.
doi:10.1016/j.polymer.2007.07.016

anhydride, epoxide and isocyanate, results in an increase in the notched impact strengths of the PET/elastomer blends from four-fold to twenty-fold that of the pure matrix. It also has been reported that only a few percents of the functionalities are found to be effective in enhancing the impact property of the blends. A few percents of these groups would be sufficient to form the cross linkage between the different phases of the system studied.

The processing condition is also a factor that is used to control morphology, which in turn will affect the mechanical properties of polymer blends. Sánchez-Solís et al. [8] demonstrated that using SBR-*g*-MA in the PET/SBR blend would enhance the impact properties of the blends. They also showed that a reduction of particle size of rubber in PET/SBR/SBR-*g*-MA blend arising from an increase of screw speed was correlated with a reduction in the shear viscosity and an increase in the impact properties of the blend.

Although, there are many publications on the compatibilization of PET with modified elastomers or polyolefin blends, no clear evidence on the interactions between the different phases have been reported. The present study concerns the investigation of PET/NR blending system using a twin-screw extruder. The effects of different blend composition and screw speed on the mechanical properties are studied without the addition of functionalized NR. Since NR is an elastomer derived from plants, it naturally possesses some abnormal groups such as epoxide, amine and hydroxyl functions as reported in the literatures [13,14]. An investigation of blend morphology as well as the molecular characteristic of the blend component would result in a better understanding of the compatibilization behaviors which affect the mechanical properties of the blends. In this study, solid-state CP/MAS ^{13}C NMR was used for this purpose.

2. Experimental

2.1. Materials

The poly(ethylene terephthalate), PET, provided by the Thai Shinkong Industry, Thailand was PET 5015w, with an intrinsic viscosity of 0.80 ± 0.02 dl/g. Its melting point is 246 ± 4 °C. The natural rubber (NR), STR 5 L grade, was supplied by Bangkok Rubber Company, Thailand.

2.2. Blend preparation

Prior to blending, the PET was dried at 120 °C for 10 h in an oven. Before blending with PET, the natural rubber (NR) was milled for 1 min at 40 °C on a two-roll mill, sheeted, and cut into small pieces. The PET and rubber were tumble mixed before feeding into a co-rotating twin-screw extruder (Prism, with a screw diameter of 25 mm, compression ratio 3:1, die diameter of 16 mm, and L/D ratio 25/1) at different screw speeds and blend compositions. The temperature profile of the twin-screw extruder was 200, 220, 230, 240, 245 °C for PET/rubber blends and the temperature profile of PET was 210, 225, 235, 245, 250 °C. The extrudate was cooled in a water bath before being cut with a granulator into pellet form.

2.3. Molding

After mixing, the blends were dried at 80 °C for 12 h before being injected. The mixed materials were molded in an injection molding machine (DR BOY 22S, 24 mm screw diameter) into tensile (width 10.0 mm, thickness 3.2 mm) and impact testing specimens (width 12.7 mm, thickness 3.2 mm). The typical operating conditions used were a 240 °C barrel temperature, a 250 °C nozzle temperature, a 50 °C mold temperature and a 150 rpm screw speed. The tensile and impact bars were stored in a desiccator until they were tested.

2.4. Mechanical testing

The tensile test, according to ASTM D638 type IV, was carried out using a Instron 5569 tensile tester with a crosshead speed of 10 mm/min at room temperature and a 5 kN load cell. A minimum of five specimens per blend composition was used to get the mean values.

All impact specimens were stored in a desiccator at least for three days after notching. Izod impact tests were carried out using a Zwick 5102 with a 2 J hammer at room temperature according to ASTM D256. All values listed are the average of the measurements done on ten samples.

2.5. Blend morphology

Scanning electron microscopy (SEM) analysis was performed on fractured surfaces with a LEO 1455VP. Samples were fractured at liquid nitrogen temperature. After the gold sputtering by a Polaron CA7625 Carbon Accessory Gold Coating, the surfaces were examined. The diameter of at least 200 particles of dispersed phase of each blend sample was determined by using the KS300.30 software developed by Kontron Elektronik GmbH.

2.6. Thermal analysis

Thermal analysis was carried out using a differential scanning calorimeter (Perkin-Elmer DSC 7). Polymer samples of 0.01 g were taken in an aluminum pan and sealed tightly with an aluminum cover. The temperature was raised from −50° to 300 °C at a rate of 20 °C/min then cooled down at a rate of 10 °C/min to −50 °C and heated up again to 300 °C at the rate of 10 °C/min. The crystallization, melting and cold crystallization temperatures symbolized as T_c, T_m and T_{cc}, respectively, were obtained. The percent crystallinity of the PET ($\%\chi_c$) in the blend was determined by using Eq. (1).

$$\%\chi_c = \frac{\left[(\Delta H_m - \Delta H_{cc})/\Delta H_m^o\right]}{\Phi_{PET}} \times 100 \quad (1)$$

where ΔH_m^o is the heat of melting of 100% crystalline PET which is 140.1 J/g [15]; Φ_{PET}, weight fraction of PET in the

blend, and ΔH_m and ΔH_{cc} are the heat of melting and cold crystallization, respectively. The values of the two heats were determined from the DSC thermograms.

2.7. Solid-state ^{13}C NMR spectroscopy

The impact bar specimen of each sample was scrubbed into a powder form by using a flat file. The samples were then packed into the ZrO_2 rotor (4 mm in diameter). Solid-state ^{13}C NMR experiments were performed at 75.47 MHz at room temperature with a BRUCKER AVANCE 300 MHz wide bore spectrometer using a cross polarization (CP)/magic angle spinning (MAS) probe. Single pulse experiments combining MAS and high power proton decoupling were carried out using a pulse width of 90° (4 μs) with a repetition time of 4 s. A spectral width of 25 kHz and 16 K data points was used for data collection. The MAS frequency was 10 kHz. The decoupling radio frequency was 60 kHz. The CP/MAS experiments were done to observe the dynamics of the PET and PET blends from the point of view of ^{13}C atoms with variable contact times, t_{cp} (0.01–20 ms). For the present research, a rotor spinning frequency of 7 kHz was used.

The reconstruction of the spectra was done with the DMFit software [16] using four adjustable parameters for each NMR line; isotropic chemical shift, linewidth, line-shape and line intensity. The ^{13}C CP magnetization curves versus contact time of each carbon of the samples were built up from the line intensities and were fitted using Origin 7.5.

3. Results and discussion

3.1. Mechanical properties of PET/NR blend

3.1.1. Influence of blend composition

PET was dried in an air oven at 120 °C for 10 h before processing in a co-rotating twin-screw extruder to avoid excessive moisture-induced degradation reactions. The notch sensitivity of semi-crystalline PET becomes quite apparent from the very low notched Izod impact strength (6.0 J/m) obtained by passing the PET in the twin-screw extruder before injection molding into test specimens. It has already been demonstrated that the impact behavior of PET can be strongly improved by rubber modification [2–7]. PET/NR blends have yet to be studied. In this study, various amounts of NR were blended with the PET in a twin-screw extruder using a screw speed of 100 rpm. Fig. 1 shows the Young's modulus and the notched Izod impact strength of PET/NR blend versus the NR content in the blend. When the NR content is increased, the impact property increases while the Young's modulus decreases. This is due to the elastomeric nature of NR and is similar to what have been reported for PET/SEBS [10] and for the amorphous copolyester/PEO-*g*-MA [17] blends.

To understand the increase of notched impact strength of PET/NR blends, we note that the brittle–transition is modified by the presence of the rubber dispersive phase. This phase can absorb and dissipate the crack energy produced. This prevents the abrupt breaking of the specimen. By increasing the rubber concentration, the acceptors of the dissipation energy are increased. This then induces a further enhancement of impact strength [18]. The Young's modulus of the blend is seen to decrease as the rubber incorporation in the PET is increased. This was most likely due to two factors: the elastomeric nature of NR in PET/NR blend and the extent of degradation of PET matrix phase [19,20]. Fox et al. [21] found a significantly greater degradation of PET occurred when it was part of a blend than that when the PET was alone, even when both were processed under similar conditions. It appears that the degradation is catalyzed by some component such as water in PET. Rigorously drying, however, did not ameliorate the reduction of degradation in the blend.

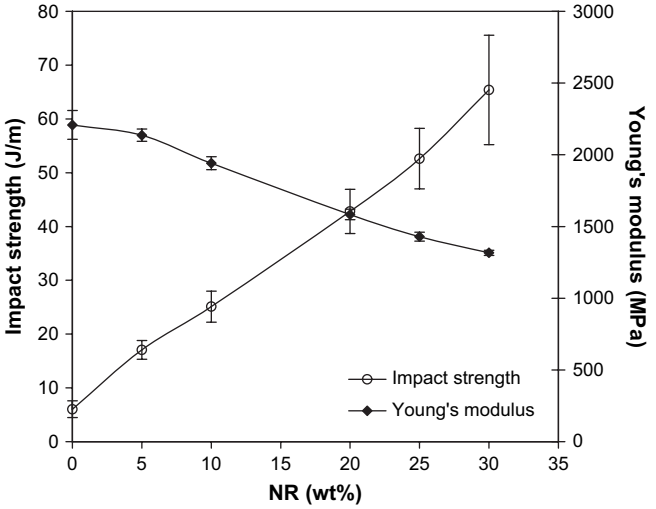

Fig. 1. Mechanical properties of PET/NR blend at various compositions at extrusion screw speed 100 rpm.

From above results, it can be summarized that when the amount of rubber in the blend increases, the Young's modulus decreased but the impact strength increased. An optimum blend composition in this study was 80/20 wt% of PET/NR blend and so it was chosen for further study of the extrusion speed that might affect its properties.

3.1.2. Influence of extrusion speed

It is well known that even without adding a third component or a compatibilizer into an immiscible blend, the processing condition will be an important factor in controlling the microstructure, the inter particle distance and the particle diameter of the disperse phase. All of these factors govern the performance of the physical and mechanical properties. Various screw speeds in extrusion process were used to process the PET/NR blends of 80/20 wt% composition. Fig. 2 shows the effect of different extrusion screw speeds (60–150 rpm) on the mechanical properties of 80/20 wt % blend. It was found that when the screw speed increased, the notched Izod impact strength and the Young's modulus did not change. This could be due to control of these properties by the injection process in the final step. This indicates that the extrusion screw speed has less effect on the mechanical properties than does the NR content in the blend.

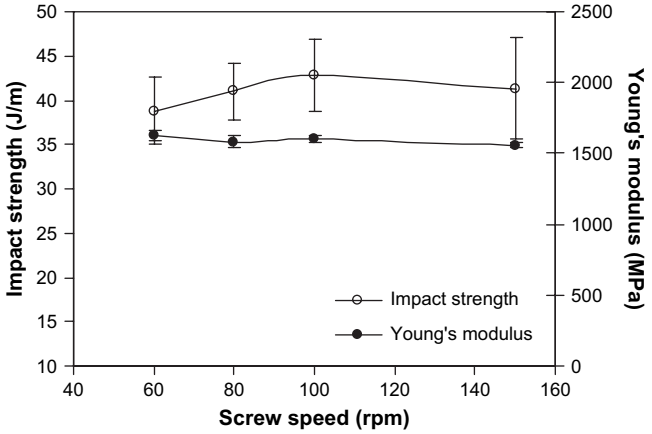

Fig. 2. Mechanical properties of PET/NR blend at 80/20 wt% at various extrusion screw speeds.

3.2. Morphology

The morphology of the injection molded specimens of the PET/NR blends was determined by the SEM. The micrographs in Fig. 3 show the outer and the inner zone of an injection molded specimen of the 80/20 wt% blend that was freezed–fractured in a transverse direction. These results reveal that the PET/NR blends exhibited a skin-core morphology similar to those seen in other rubber modified PET system such as PET/SEBS [10,22], PBT-Ph/*m*PEO [23] or PBT/PEO [24]. The holes near the edge of the sample containing the NR domains are elongated NR of predominantly rod-shapes as shown in Fig. 3a. A few holes were oval, suggesting that some of the elongated NR domains were slightly flattened just as seen in PET/SEBS-*g*-MA blend [10,22] and PBT/PEO blend [25]. The morphology of the core, seen in Fig. 3b, consists of spherical domains of 1.5 μm diameter. The outer layer is not discussed here since it was very thin (about 100–150 μm). As a consequence of its thinness, it would have negligible influence on the mechanical properties. Only the morphological data of the inner part of the specimens are considered in this study. Fig. 4 shows the SEM micrographs of various blends' ratio of PET/NR. The particle sizes of the rubber in the blends and its impact strength are plotted with the blend composition as shown in Fig. 5. It was found that the average particle size did not increase linearly with the amount of the added rubber. The average particle diameter of about 1.4 μm was obtained when 5% of rubber was added. This value was relatively constant up to 20% of rubber content added. The average particle size increased again when the amount of rubber was increased to 25%. It remained constant as the amount of rubber was increased to 30%. The binary PET/NR blends displayed very coarse phase morphology with large average particle sizes of about 2.8 μm. This is due to the coalescence of NR at high rubber content. The large particle sizes are expected because of the higher viscosity ratio (η_{NR}/η_{PET}) and the high interfacial tension (σ) between the two phases.

The SEM micrographs of the cryogenic fractured surface of PET/NR blends at various screw speeds were also investigated. Plots of the average particle diameters versus the impact strength of the blend with various screw speeds in extrusion process are shown in Fig. 6. It is seen that the smallest particle size of the rubber particle (1.46 μm) dispersed in PET gave the highest impact strength of the blend (43 J/m). It could be also noted that the PET/NR blend processed at 150 rpm had relatively high impact strength even though the rubber particle size was 2.2 μm, similar to the results shown in Fig. 5. Therefore, in the blends studied, the size of rubber dispersed phase is not the key factor in controlling the mechanical properties of the blends.

3.3. Thermal properties

Since PET is semi-crystalline polymer, the incorporation of the rubber in the PET could affect the crystallinity of the plastic. This could have influence on the mechanical properties of the blend. The DSC heating thermograms normally provide information on the phase structures of the PET and its blends; i.e., melting temperature (T_m), cold crystallization temperature (T_{cc}), and crystallization temperature (T_c). We have therefore obtained the heating thermograms of NR, PET and PET/NR blended at 80/20 wt%. These are compared in Fig. 7. The samples were almost amorphous as indicated by well-defined glass transition temperature and large cold crystallization exotherm. The transition temperature at −67 and 84 °C in Fig. 7a and b, were related to the glass transition temperature of NR and PET, respectively. The endotherm peak at 248.5 °C is due to

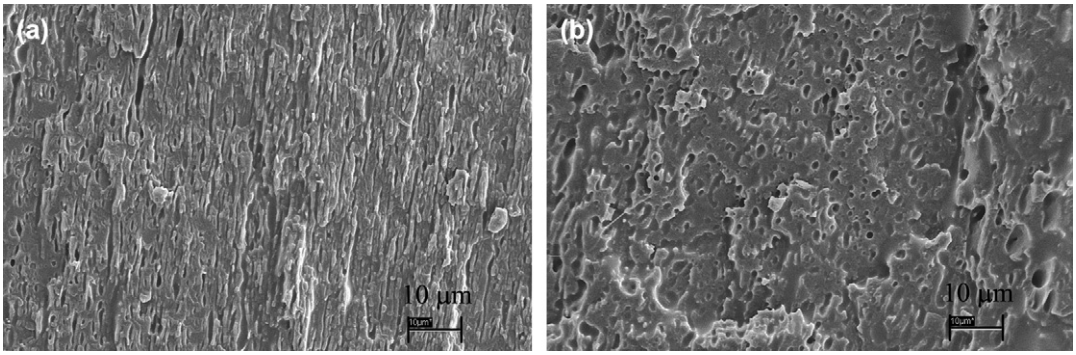

Fig. 3. Cryofracture surfaces of the (a) outer and (b) inner zone of injection molded impact specimens of PET/NR 80/20 wt%.

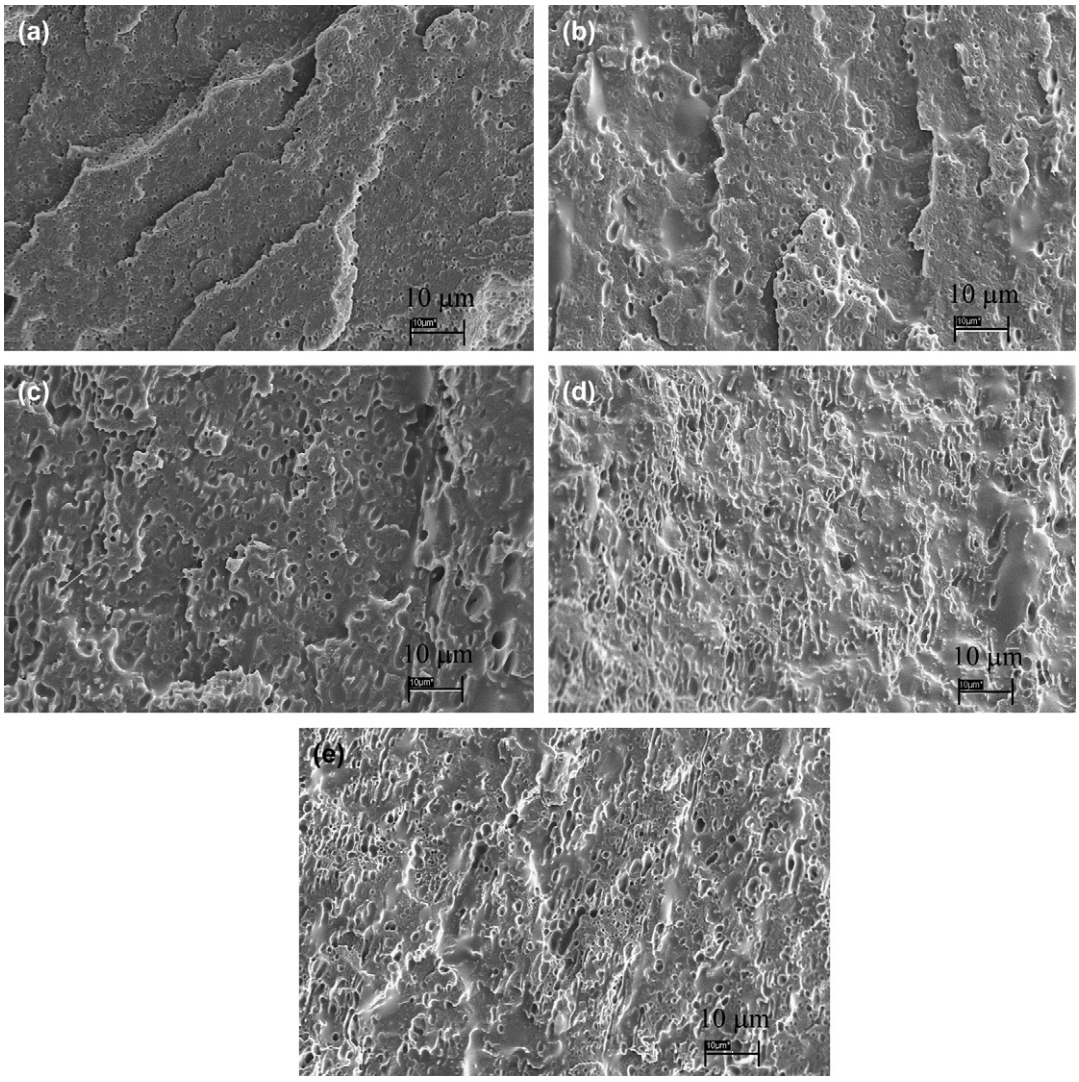

Fig. 4. Cryofracture surfaces of the inner zone of the injection molded impact specimens of PET/NR blends at (a) 95/5, (b) 90/10, (c) 80/20, (d) 75/25 and (e) 70/30 wt%.

the melting of PET (T_m). The exotherm peak at 171.2 °C is a result of cold crystallization of PET (T_{cc}). The data from the DSC thermograms of PET/NR blend at various blend compositions are summarized in Table 1. The T_m of PET in PET/NR blend at 80/20 wt% occurs at a similar position as that of pure PET. This temperature indicated that the PET/NR are

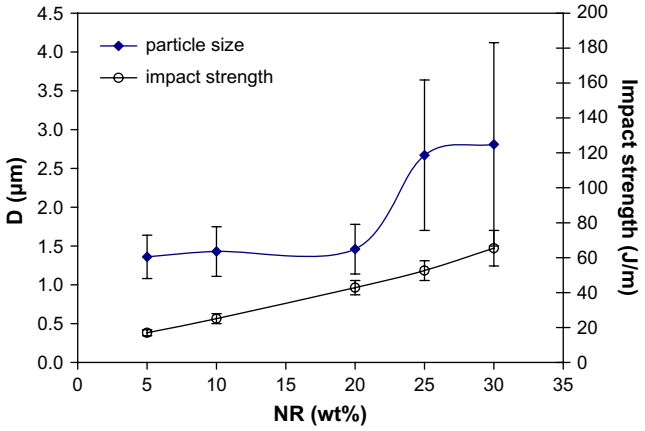

Fig. 5. Particle size and impact strength of PET/NR blend as a function of natural rubber dispersed phase content at screw speed 100 rpm.

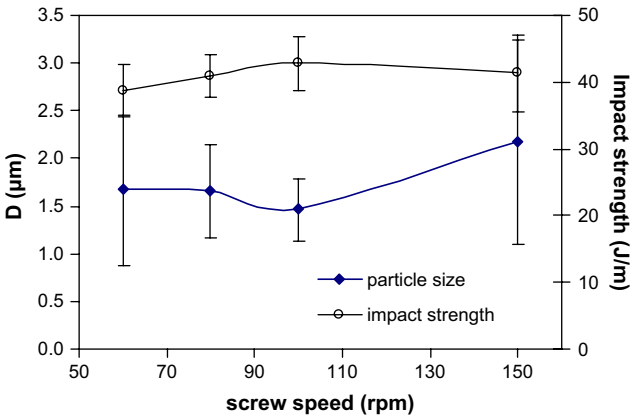

Fig. 6. Particle size and impact strength of PET/NR 80/20 wt% as a function of extrusion screw speed.

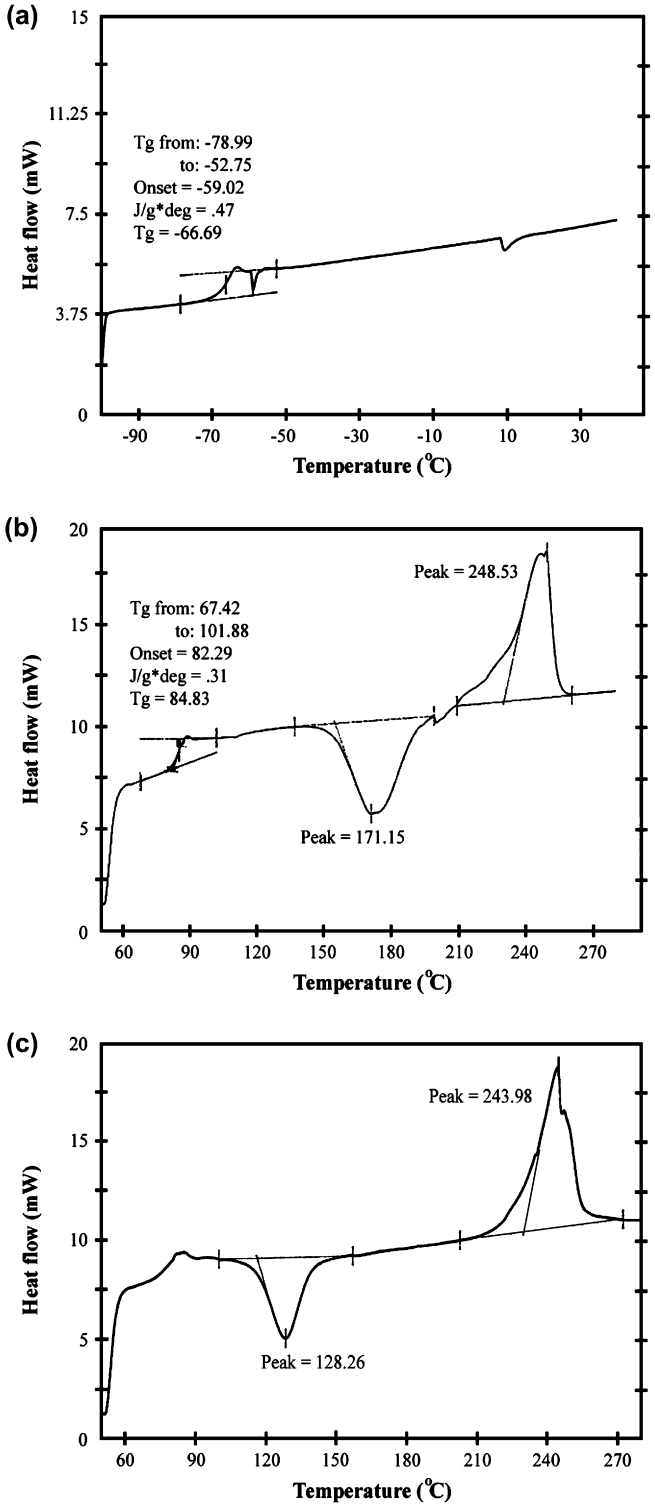

Fig. 7. DSC heating thermograms of (a) NR, (b) PET and (c) PET/NR 80/20 wt%.

not compatible. This conclusion is supported by the scanning electron micrographs (see Fig. 3).

The percentage of crystallinity of the PET in the PET/NR blend ($\%\chi_c$) was determined by using Eq. (1). It can be seen in Table 1 that the crystallinity of the PET/NR blend significantly changed from that of pure PET. By increasing the rubber portion in the blend, the percent crystallinity of the PET is increased. The rubber could be acting as a nucleating agent in the PET matrix, causing an approximately 40 °C lowering of the T_{cc} of PET. The decrease of the T_{cc} of the PET has also been found in PET/SEBS-*g*-MA [10].

Table 1
DSC results of PET/NR blends at various blend compositions

PET/NR	T_{cc} (°C)	T_m (°C)	ΔH_{cc} (J/g)	ΔH_m (J/g)	T_c (°C)	$\%\chi_c$
100/0[a]	171.2	248.5	25.01	31.11	–	4.35
90/10	123.4	246.3	24.24	38.15	176.2	11.03
80/20	128.3	244.0	15.50	32.94	185.7	15.56
70/30	124.6	243.3	10.04	30.28	185.9	20.64

[a] PET as received.

The thermal behavior of the PET/NR 80/20 wt% blends at various extrusion screw speeds were investigated by the DSC technique. The results are given in Table 2. It is seen that increasing the screw speed does not affect the T_m, and T_c of the PET in the blend. The 80/20 wt% PET/NR processed at the various speeds had similar percent crystallinity. This indicated that the crystallization of PET/NR blend is not controlled by the screw speed in extrusion process.

3.4. Molecular characterization of PET/NR blend

The PET and its blend are solid materials and are insoluble at room temperature in organic solvent. Then analysis of the molecular characteristic in solid form can be done by solid-state ^{13}C NMR spectroscopy. In this study, the molecular characteristics of PET and PET/NR blend were investigated by using a solid-state ^{13}C NMR with MAS and CP/MAS instrument.

3.4.1. Molecular characteristic of PET

The solid-state CP/MAS ^{13}C NMR spectrum of PET sample is shown in Fig. 8. Three main peaks are observed, i.e., singlet (61 ppm), doublet (129 and 133 ppm) and singlet (164 ppm) which are assigned to methylene, aromatic carbons and carbonyl carbon of PET, respectively. Furthermore, the spinning side bands of these peaks appear as small peaks, denoted by an asterick (*) in Fig. 8.

In order to get more information on the molecular structure and the dynamic properties of the material, cross polarization (CP) experiments were carried out at various contact times. It can be seen from Fig. 9 that the intensities of the signals in the solid-state ^{13}C NMR spectra of PET change significantly when the contact time is varied from 0.01 to 20 ms. At the smallest contact time (0.01 ms), only the resonance signals

Table 2
DSC results of PET/NR 80/20 wt% at various extrusion screw speeds

Screw speed (rpm)	T_{cc} (°C)	T_m (°C)	ΔH_{cc} (J/g)	ΔH_m (J/g)	T_c (°C)	$\%\chi_c$
60	124.4	244.4	16.34	33.95	186.8	15.71
80	127.3	245.6	17.21	34.25	184.0	15.20
100	128.3	244.0	15.50	32.94	185.7	15.56
150	128.5	245.2	16.25	33.87	185.9	15.72

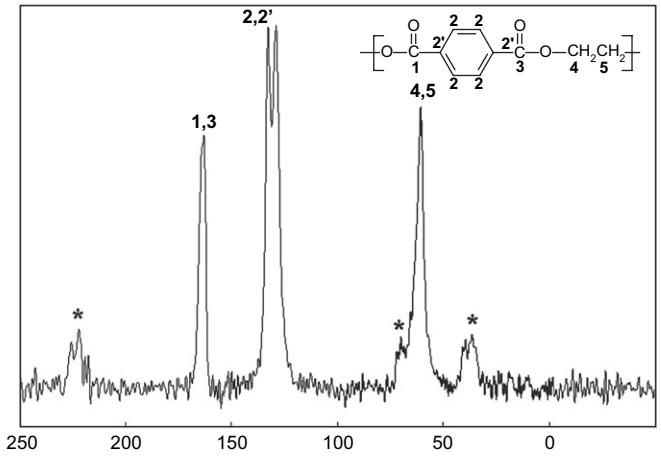

Fig. 8. CP/MAS ^{13}C NMR spectrum of PET sample.

at 61 and 129 ppm are observed. These peaks are related to the methylene and aromatic carbons (position 2), respectively. The result reflects that the peaks correspond to large dipolar $^{1}H-^{13}C$ interactions. The resonances of carbonyl (164 ppm) and aromatic (position 2′ at 133 ppm) carbons appear at 0.1 ms and the intensity of these peaks progressively increases at longer contact times owing to the smaller dipolar $^{1}H-^{13}C$ interactions. For each contact time, the ^{13}C NMR spectrum was further reconstructed by using the DMfit software [16] to determine the peak positions and intensities.

The different carbon peak intensities are plotted versus the contact time values in Fig. 10. In conventional CP process under Hartmann–Hahn conditions, ^{1}H and ^{13}C spin systems are spin-locked in rotating frames and thermally in contact with each other, thus exchanging their energies. The curves are directly related to the dynamics of the process of cross polarization. They can then be interpreted using several models [26]. When the $^{1}H-^{1}H$ interactions far exceed the heteronuclear dipolar coupling constants, the magnetization transfer is comparable to a relaxation process which is incoherent. The

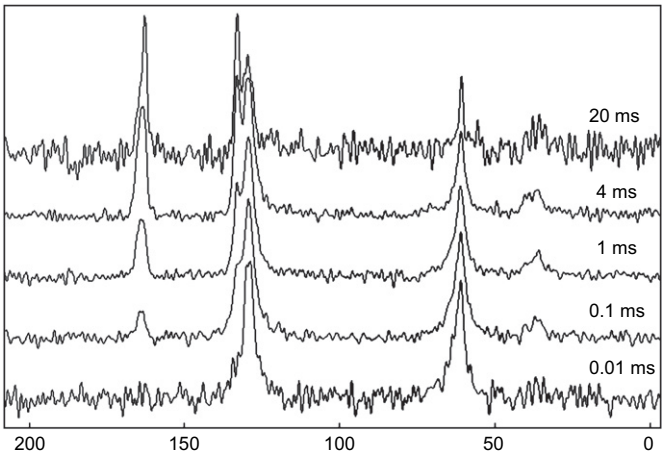

Fig. 9. Stack plots of solid-state ^{13}C NMR spectra of PET at various contact times (0.01–20 ms).

^{13}C magnetization is characterized by two time constants as follows:

$$M(t_{cp}) \propto \frac{1}{1-\lambda}\left[1-\exp\left\{-(1-\lambda)\frac{t_{cp}}{T_{CH}}\right\}\right]\exp\left\{-\frac{t_{cp}}{T_{1\rho}^{H}}\right\} \quad (2)$$

The t_{cp} corresponds to the contact time, M corresponds to the ^{13}C Zeeman magnetization, $\lambda = \frac{T_{CH}}{T_{1\rho}^{H}}$ where T_{CH} stands for the cross relaxation time and $T_{1\rho}^{H}$ is the relaxation time of protons in the rotating frame. This is called the I-S model [26].

When the $^{13}C-^{1}H$ dipolar interaction is comparable to the $^{1}H-^{1}H$ interactions, the above equation can hold no longer. This condition is true for rigid CH_n groups. The CP is no longer a single exponential process but proceeds in two stages with quite different time scales and a quantitative expression for this is given by the following

$$M(t_{cp}) \propto \left[1-s\exp\left\{-\frac{t_{cp}}{T_D}\right\}-(1-s)\exp\left\{-\frac{3}{2}\frac{t_{cp}}{T_D}\right\} \times \exp\left\{-\frac{1}{2}\frac{t_{cp}^2}{T_C^2}\right\}\right]\exp\left\{-\frac{t_{cp}}{T_{1\rho}^{H}}\right\} \quad (3)$$

where $s = \frac{1}{1+n}$ and n corresponds to the number of directly bonded protons. T_C accounts for the coherent transfer of magnetization involving the ^{13}C nucleus and the directly bonded protons, T_D is related to the spin diffusion process which involves all remaining protons. As usually $T_D \gg T_C$, the transfer of magnetization occurs first between the ^{13}C nuclei and the neighbouring protons and then with the more remote protons. This is called the I-I*-S model [26].

It was impossible to describe the experimental data using Eq. (2). The opposite is true with Eq. (3). We find that the fit derived from Eq. (3) is in good agreement with the experimental data (the calculated curves are shown as a solid line in Fig. 10). The fit gives us the characteristic values of T_C, T_D, $T_{1\rho}^{H}$, s (Table 3).

It can be seen that at the beginning of the curve, the intensity of the peak progressively increases and reaches a maximum prior to decreasing with increasing contact time. The increase in the ^{13}C intensities at short contact time is dominated by the CP rate ($1/T_C$), whereas the slow rise in the intensity is controlled by T_D. The decrease in the intensity for the longer contact times is dominated by the ^{1}H spin lattice relaxation rate in the rotating frame ($1/T_{1\rho}^{H}$).

The results are in agreement with the well known behavior: the larger the number of ^{1}H nuclei bonded (and close) to the analysed ^{13}C nucleus, the more rigid the C–H bond, the stronger and faster the transfer. Thus, for the C_4 and C_5 carbons of the CH_2 groups ($s = 0.30$) and for the aromatic C_2 carbon ($s = 0.41$), the magnetization transfer is faster than for the quaternary carbonyl carbons $C_{1,3}$ ($s = 0.92$) and the aromatic $C_{2'}$ carbon ($s = 0.85$).

It can be noticed that $T_{1\rho}^{H}$ relaxation time of methylene carbon of PET has value in the same range with $T_{1\rho}^{H}$ relaxation times of aromatic carbon and carbonyl carbon (10.5–11 ms).

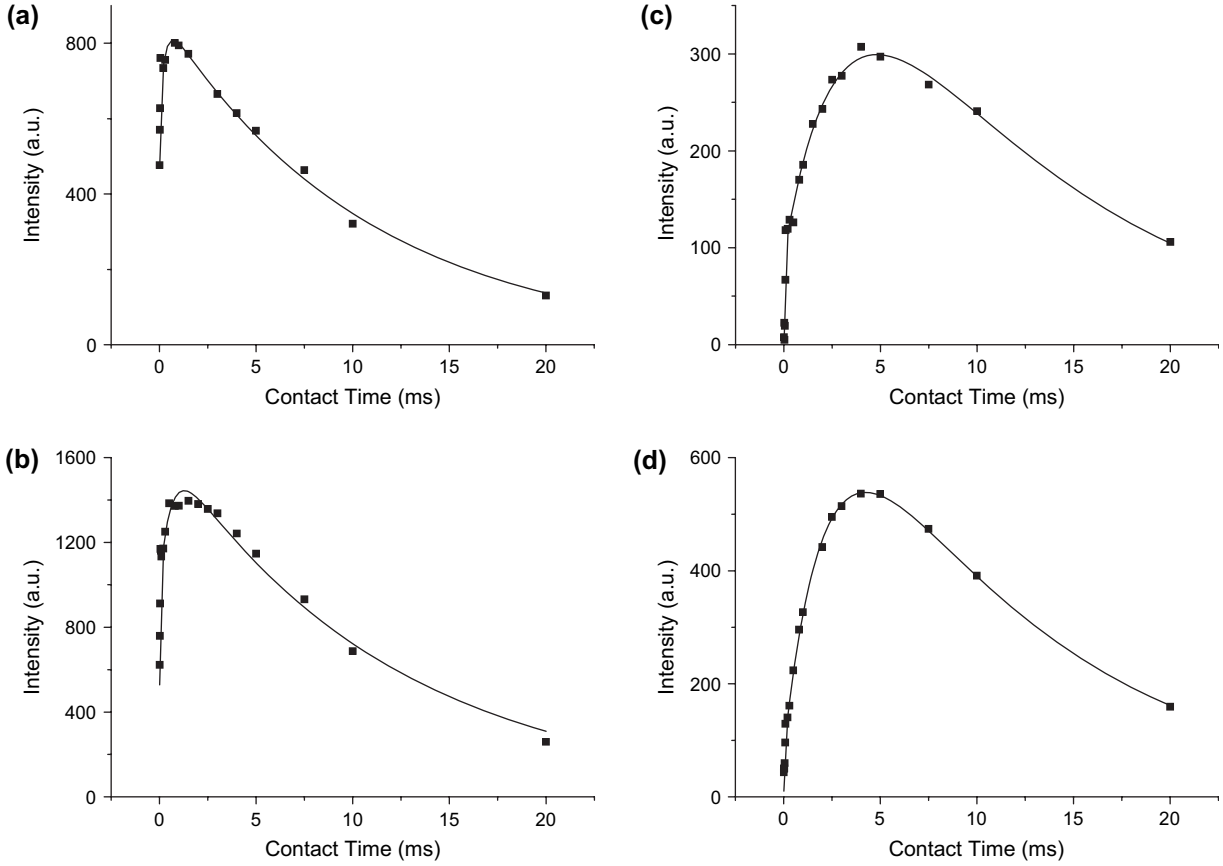

Fig. 10. Plot of normalised intensity with contact times of PET sample taken at (a) 61 ppm, (b) 129 ppm, (c) 133 ppm and (d) 164 ppm.

This result shows that spin diffusion is quite efficient leading to a unique H reservoir and a unique rotating frame spin lattice relation. This is in agreement with a high rigidity of the PET network.

In addition, the cross polarization time (T_C) of aromatic carbon (at 133 ppm) and carbonyl group (at 164 ppm) has a remarkably higher value than that of aromatic carbon (at 129 ppm) and methylene carbon (at 61 ppm).

From the above results, the *s* values can be used to infer the trend of amount of protons (*n*) directly bonded to the studied carbon. The *n* values for methylene (at 61 ppm), aromatic carbon (at 129 ppm), aromatic carbon (at 133 ppm), and carbonyl carbon (at 164 ppm) are 2.3, 1.4, 0.2 and 0.1, respectively.

3.4.2. Molecular characteristic of PET/NR blend

In the case of PET/NR blend, it was found that the impact strength of this blend was higher than the pure PET. It is proposed that the NR have some physical or chemical bonding with the PET.

Table 3
Typical data of curve fitting of PET spectra

Position (ppm)	*s*	T_C (μs)	T_D (ms)	$T_{1\rho}^H$ (ms)
61	0.30 ± 0.04	6.2 ± 0.7	0.3 ± 0.1	10.7 ± 1.1
129	0.41 ± 0.04	8 ± 1	0.9 ± 0.4	10.5 ± 1.2
133	0.85 ± 0.04	53 ± 8	4.3 ± 1.6	11 ± 2
164	0.92 ± 0.01	24 ± 5	2.8 ± 0.4	11 ± 1

Solid-state ^{13}C NMR spectra of PET/NR blend at 80/20 wt% are shown in Fig. 11. The sharp resonance peaks of NR were detected by using MAS technique (Fig. 11a) while the broad resonance peaks assigned to PET molecular characteristic were observed by using CP/MAS technique (Fig. 11b). In the case of NR portion, Fig. 11a shows three peaks at 23, 26 and 32 ppm which can be assigned to methyl carbon and two methylene carbons of NR, respectively. Two more peaks at 125 and 134 ppm were observed and assigned to olefinic carbons of NR. By using CP/MAS technique, the NMR spectrum of the PET portion (Fig. 11b) presented a singlet at 61 ppm, a doublet at 129 and 133 and a singlet at 164 ppm. These were assigned to methylene, aromatic and carbonyl carbon, respectively.

Further analysis of the molecular characteristic of the PET/NR blend was carried out by varying the contact time. The stack plots of solid-state ^{13}C NMR spectra of PET/NR 80/20 wt% with the contact time ranged from 0.01 to 20 ms are shown in Fig. 12. Similar to the case of pure PET, it can be seen that at the lowest contact time (0.01 ms), two significant peaks were observed at 61 and 129 ppm. These are assigned to the resonance of the methylene and aromatic carbons corresponding to large dipolar $^1H-^{13}C$ interactions. The carbon resonance of carbonyl (164 ppm) and aromatic groups (133 ppm)

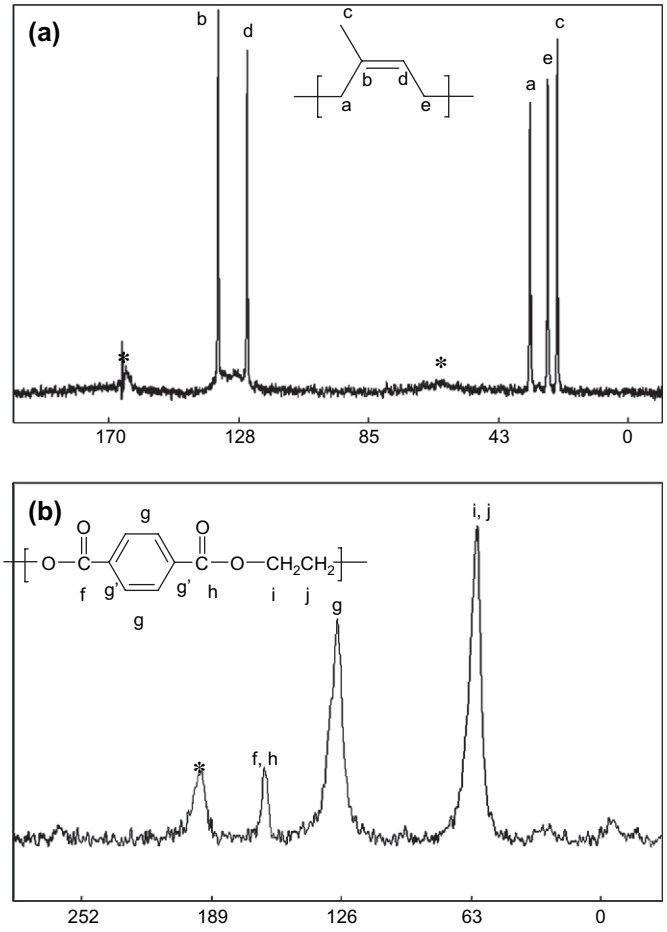

Fig. 11. ^{13}C NMR spectra of (a) NR part and (b) PET part in PET/NR blend at 80/20 wt%.

appears at longer contact time and their intensities were progressively increasing for longer contact times.

For each contact time, the ^{13}C NMR of PET/NR 80/20 wt% blend spectrum (as shown in Fig. 12) was reconstructed with the DMfit software [16]. The different carbon peak intensities versus the contact time values are shown in Fig. 13. Their behavior is quite similar to that observed for pure PET. The I-I*-S model (Eq. (3)) was again used to fit the intensity curves. The results are shown as solid lines in Fig. 13. The different parameters obtained from the fitted curves are given in Table 4. Compared to the PET, in PET/NR blend, the $T_{1\rho}^{H}$ relaxation time is smaller for the carbonyl group at 164 ppm (8.3 ms), and the methylene carbon at 61 ppm (8.7 ms). Owing to the experimental errors, no definite conclusion can be drawn for the aromatic carbon at 133 and 129 ppm. The smaller $T_{1\rho}^{H}$ indicates a faster proton relaxation in the rotating frame. This may be tentatively related to the possible interaction occurring between the PET and the NR chains near the carbonyl or the methylene positions, which slightly affects the molecular mobility of PET in the kHz range. It has been reported that the molecular chain of NR contains some abnormal groups such as epoxide, amine and hydroxyl functions [13,14]. The epoxide concentration was reported to be about 0.53 mol% and the amount of amine (or hydroxyl) was found to be a half of epoxide content [13]. It had been reported that the compatibility of thermoplastic polyurethane elastomer and polyethylene blend as well as its properties could be improved when the polyethylene was grafted with 0.5 wt% maleic anhydride [27]. Therefore, it could be postulated that the presence of a small amount of hydroxyl function of NR would interact with the carbonyl group of PET via hydrogen bonding as shown in Fig. 14.

Also, the spin diffusion time T_D of the carbonyl group is larger in PET/NR blend (3.9 ms) than that in PET (2.8 ms). This would correspond to a slower spin diffusion rate. This indicates that cross polarization at the carbonyl group in the blend is less efficient than that in the PET, corresponding to more mobile remote protons. Within the error range, the other relaxation times are unaffected. This confirms that an interaction between the carbonyl group of PET and abnormal groups such as hydroxyl function of NR might be occurring.

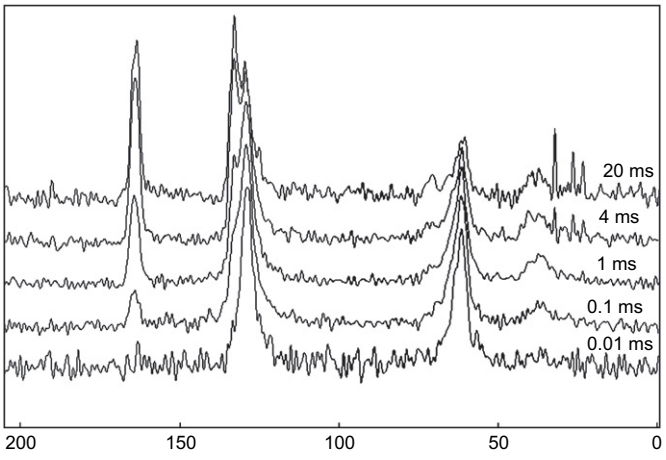

Fig. 12. Stack plots of solid-state ^{13}C NMR spectra of PET/NR 80/20 wt% at various contact times (0.01–20 ms).

4. Conclusion

Toughened PET can be obtained by the addition of NR using twin-screw extruder. This investigation clearly revealed that both the mechanical properties, e.g., Young's modulus and impact strength as well as the morphological characteristic of the PET/NR blend are influenced by the amount of rubber and processing condition. The high impact strength values were obtained without prior chemical modification of the NR. The Solid-state CP/MAS ^{13}C NMR spectroscopy revealed that the interaction between the PET and the NR occurred though the observation of an increase in cross polarization time (T_D) of the carbonyl carbon and a decrease of $T_{1\rho}^{H}$ relaxation of the carbonyl group in the PET/NR blend. This should come from the interaction between the carbonyl group of PET with the abnormal groups such as hydroxyl function in NR, resulting in improving the compatibility of the studied blends, hence increasing the toughness.

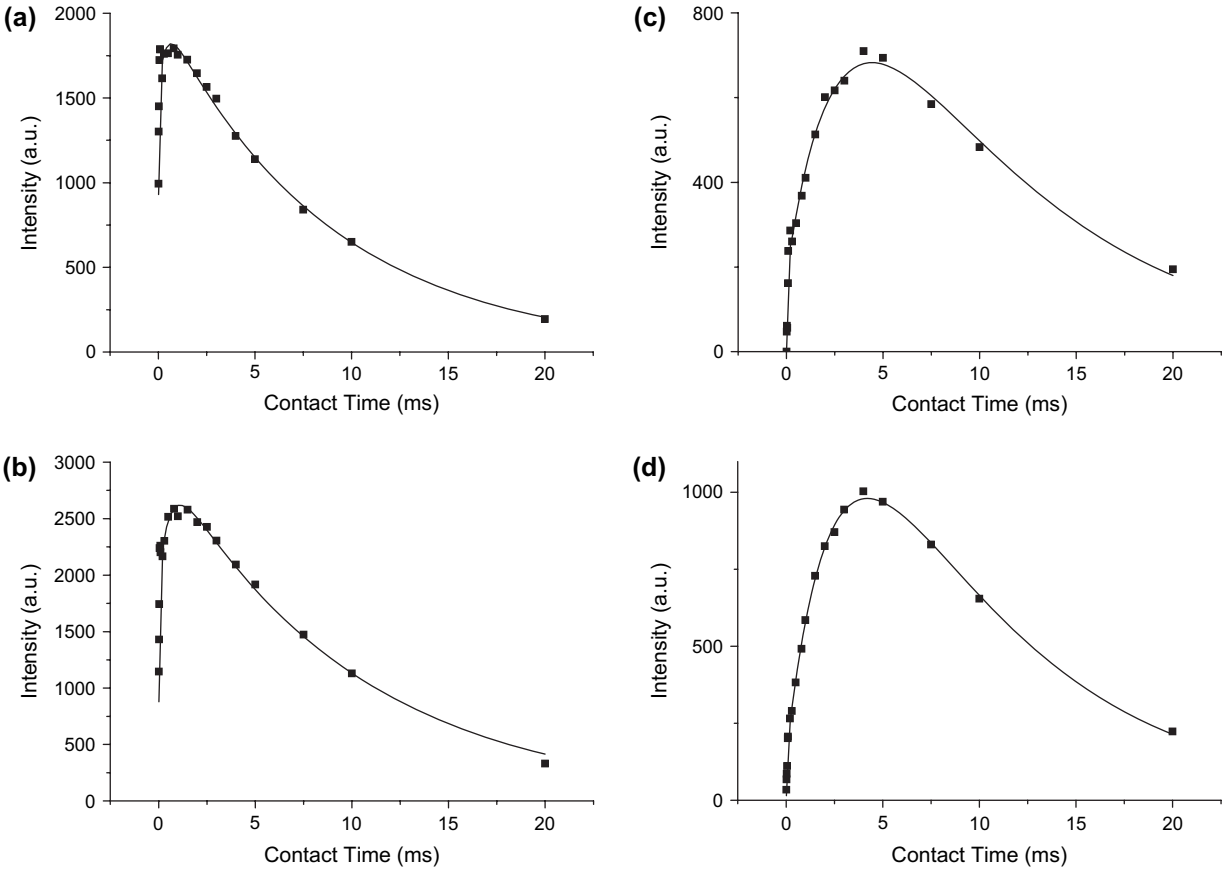

Fig. 13. Plot of normalised intensity with contact times of PET/NR 80/20 wt% taken at (a) 61 ppm, (b) 129 ppm, (c) 133 ppm and (d) 164 ppm.

Table 4
Typical data of curve fitting of spectra of PET/NR 80/20 blend

Position (ppm)	s	T_C (μs)	T_D (ms)	$T_{1\rho}^H$ (ms)
61	0.25 ± 0.04	7.6 ± 0.7	0.4 ± 0.2	8.7 ± 0.9
129	0.38 ± 0.04	9 ± 1	0.6 ± 0.2	10 ± 1
133	0.89 ± 0.03	48 ± 8	4.5 ± 1.7	9.0 ± 1.6
164	0.94 ± 0.01	29 ± 4	3.9 ± 0.5	8.3 ± 0.6

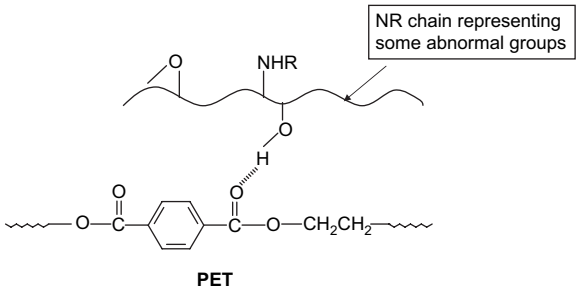

Fig. 14. Proposed interaction via hydrogen bonding between the carbonyl group of PET with abnormal groups such as hydroxyl function in NR.

Acknowledgements

The authors would like to thank the Thailand Toray Science Foundation for partial financial support for this work. The scholarship from the Institutional Strengthening Program, Faculty of Science, Mahidol University, Thailand to J. Saelao is also appreciated. Special thank also goes to Prof. Philippe Daniel, Laboratoire de Physique de l'Etat Condensé, Faculté des Sciences, Université du Maine, France for providing short stay of J. Saelao at Université du Maine, France.

References

[1] Bucknall CB. Toughened polymers. Applied Science Publishers; 1977.
[2] Loyens W, Groeninckx G. Polymer 2003;44(1):123–36.
[3] Chapleau N, Huneault MA. J Appl Polym Sci 2003;90:2919–32.
[4] Mouzakis DE, Papke N, Wu JS, Karger-Kocsis J. J Appl Polym Sci 2001;79(5):842–52.
[5] Papke N, Karger-Kocsis J. Polymer 2001;42(3):1109–20.
[6] Loyens W, Groeninckx G. Macromol Chem Phys 2002;203(10–11):1702–14.
[7] Al-Malaika S, Kong W. Polymer 2005;46:209–28.
[8] Sánchez-Solís A, Calderas F, Manero O. Polymer 2001;42(17):7335–42.
[9] Loyens W, Groeninckx G. Polymer 2002;43(21):5679–91.
[10] Fung KL, Li RKY. Polym Test 2005;24:863–72.
[11] Paul S, Kale DD. J Appl Polym Sci 2001;80(13):2593–9.
[12] Tanrattanakul V, Hilter A, Baer E. Polymer 1997;38(9):2191–200.
[13] Burfield DR, Chew LC, Gan SN. Polymer 1976;17:713–6.
[14] Eng AH, Tangpakdee J, Kawahara S, Tanaka Y. J Nat Rubb Res 1997;12(1):11–9.
[15] Sichina WJ. DSC as problem solving tool: measurement of percent crystallinity of thermoplastics. Application notes for thermal analysis. PerkinElmer, http://www.perkinelmer.com; 2000.
[16] Massiot D, Fayon F, Capron M, King I, Le Calvé S, Alonso B, et al. Magn Reson Chem 2002;40:70–6.

[17] Yu ZZ, Lei M, Ou YC, Yang G, Hu GH. J Polym Sci Part B Polym Phys 2000;38(21):2801–9.
[18] Collyer AA. Rubber toughened engineering plastics. London: Chapman and Hill; 1994.
[19] Andrassy M, Mencer HJ. Polym Degrad Stab 1993;41(1):77–81.
[20] Mantia FPL, Vinci M. Polym Degrad Stab 1994;45(1):121–5.
[21] Fox B, Moad G, van Diepen G, Willing I, Cook WD. Polymer 1997;38(12):3035–43.
[22] Pawlak A, Perkins WG, Massey FL, Hiltner A, Baer E. J Appl Polym Sci 1999;73(2):203–19.
[23] Aróstegui A, Nazábal J. Polymer 2003;44(1):239–49.
[24] Aróstegui A, Nazábal J. J Appl Polym Sci 2004;91(1):260–9.
[25] Aróstegui A, Gaztelumendi M, Nazábal J. Polymer 2001;42(23): 9565–74.
[26] Kolodziejski W, Klinowski J. Chem Rev 2002;102(3):613–28.
[27] Potschke P, Wallheinke K, Stutz H. Polym Eng Sci 1999;39:1035–48.